

Supporting information

Oxygen Vacancy-Enriched NiO Nanozymes Achieved by Facile Annealing in Argon for Detection of L-Cys

Sihua Wu,^a Jinhui Zou,^a Baohua Zhang,^{*a,b} Jiantian Lu,^a Guanrong Lin,^a Yuwei Zhang ^{*a,c} and Li Niu^{a,d}

^a Guangzhou Key Laboratory of Sensing Materials & Devices, Center for Advanced Analytical Science, School of Chemistry and Chemical Engineering, Guangzhou University, Guangzhou 510006, China. E-mail: ccbhzhang@gzhu.edu.cn

^b State Key Laboratory of Organic Electronics and Information Displays & Institute of Advanced Materials (IAM), Nanjing University of Posts & Telecommunications, Nanjing, 210023, China

^c GDMPA Key Laboratory for Process Control and Quality Evaluation of Chiral Pharmaceuticals, Guangzhou Key Laboratory of Analytical Chemistry for Biomedicine, School of Chemistry, South China Normal University, Guangzhou 510006, China. E-mail: ywzhang@scnu.edu.cn

^d Sun Yat Sen University, School of Chemical Engineering and Technology, Zhuhai 519000, China.

Corresponding Author

*(B.Z.) E-mail: ccbhzhang@gzhu.edu.cn

*(Y.Z.) E-mail: ywzhang@scnu.edu.cn

1. Supplementary Figures

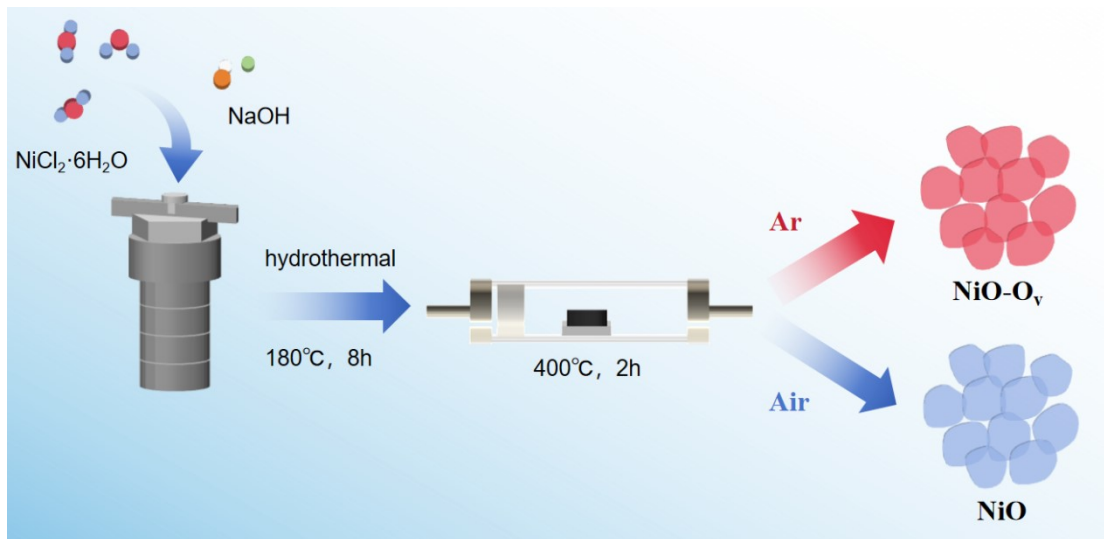


Figure S1. The synthetic route of NiO an NiO-Ov samples.

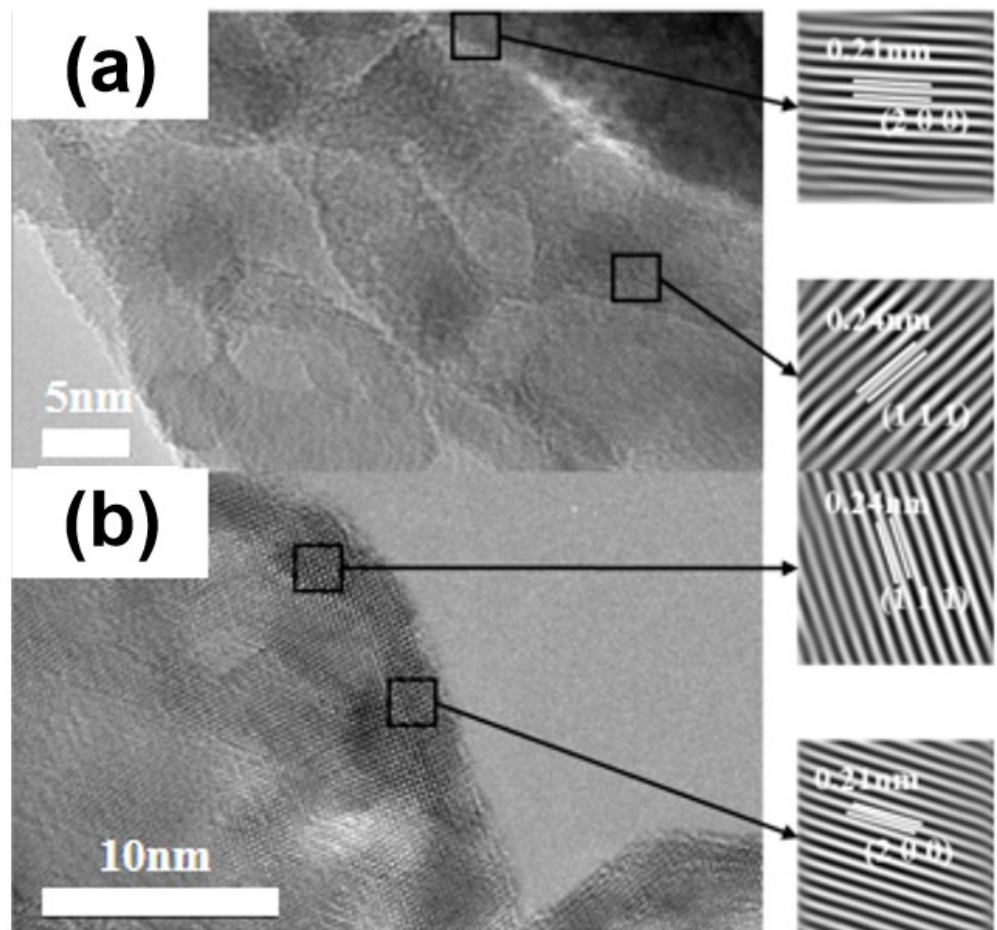


Figure S2. High-resolution TEM of (a) NiO; (b) NiO-Ov (The black boxes correspond to the Fourier-transformed lattice stripes)

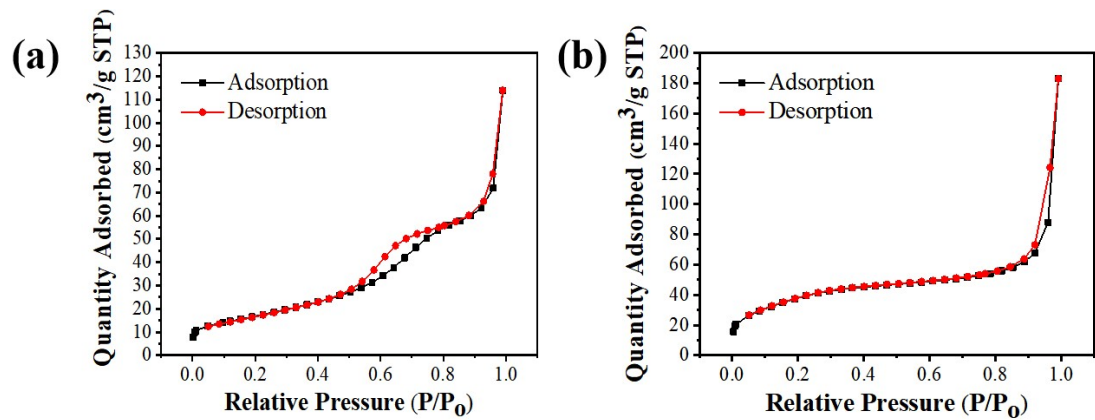


Figure S3. BET test curve comparison: (a) NiO; (b) NiO-OV.

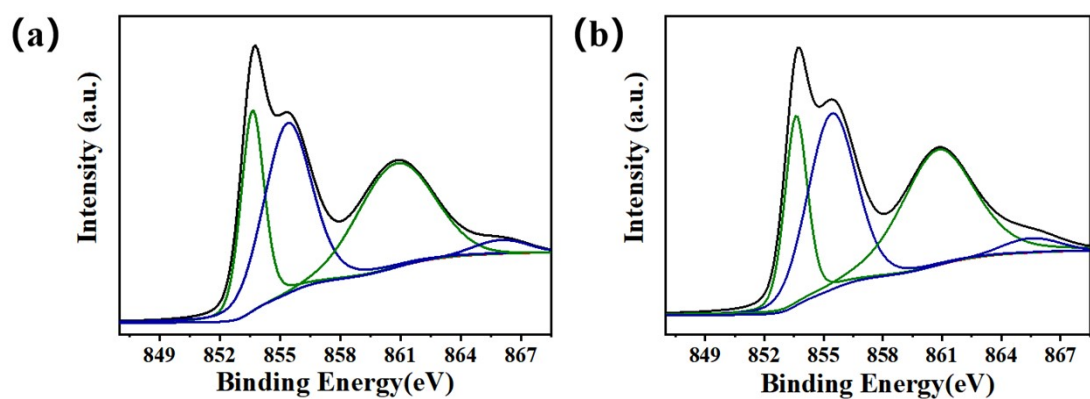


Figure S4. XPS spectra of different samples of Ni2p: (a) NiO; (b) NiO-O_v.

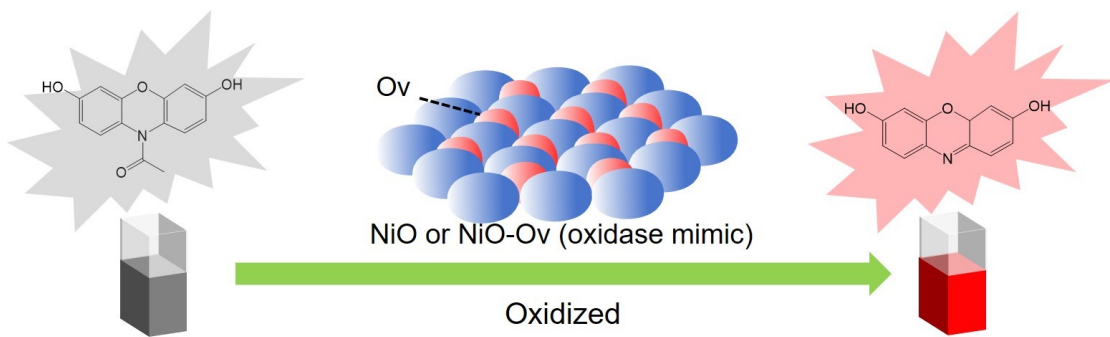


Figure S5. Schematic diagram of Fluorescent turn-on process for catalysis of NiO or NiO-Ov nanozyme on AR to resorufin.

2. Supplementary Tables

Table S1. Structural parameters of NiO samples calcined in different atmospheres

Sample	2θ (°)	FWHM	Grain size ^a (nm)	BET ^b (m ² /g)	Pore size (nm)
NiO	43.240	0.641	2.97	62.01	9.39
NiO-O _V	43.220	0.820	2.32	136.55	12.37

^a calculated by the method of Scherrer's equation based on the diffraction of the (200) peak of NiO at 2θ = 43.1°.

^b calculated by the method of specific surface area.

Table S2. The summary of XPS results of different NiO samples.

Sample	Binding energy (eV)				Atomic ratio(%)		EPR area	
	Ni 2p _{3/2}		O 1s			Ni ³⁺ / Ni ²⁺		
	Ni ²⁺	Ni ³⁺	O _a	O _β	O _γ			
NiO	853.6	855.43	529.15	531.18	532.14	1.72	21.4	8.1×10 ⁴
NiO-O _V	853.63	855.45	529.18	531.08	532.91	1.85	32.8	1.1×10 ⁵

Table S3. Comparison of kinetic parameters (K_m and V_{max}) corresponding to different nanozymes

Substrate	Nanozymes	K_m (μM)	V_{max} (nM s^{-1})	Ref.
Amplex Red	Bi–Au NPs	89.3	15.0	1
	ZiF-67	5.28	28.2	2
	FeP@C	2.30	—	3
	Au/AgCl	17	4.6	4
	MFNP1:1	34.2	244	5
	CoOxH-GO	4.87	0.839	6
	NiO-O _V	2.83	26.7	this work

Table S4. Detection range and detection limit of L-Cys by different systems

System	Method	Linear range (μM)	Detection limit (nM)	Ref.
Co_4S_3	fluorescence	0.25-2.5	75	7
AuNRs/Au-Ag NCs	fluorescence	5-100	1.73×10^3	8
AuNCs-AuNPs	fluorescence	1.5-35	1.4×10^3	9
Si-CDs	fluorescence	20-100	410	10
CDs	chemiluminescence	10-100	8.8×10^3	11
$\text{OV}-\text{Mn}_3\text{O}_4$	colorimetric	5-800	1.31×10^3	12
$\text{Gd}(\text{OH})_3$	colorimetric	0.2-75	2.6×10^3	13
2D Co_3S_4	colorimetric	0.2-100	2.7×10^3	14
VS_4	colorimetric	5-100	2.5×10^3	15
$[\text{Ag}_2(\text{bit})_2]_2[\text{Mo}_8\text{O}_{26}]$	colorimetric	1-100	220	16
rGO-GP	colorimetric	2-30	100	17
MnO_2 nanobelts	colorimetric	0-35	100	18
$\text{MnO}_2@\text{Co}_3\text{O}_4$	colorimetric	1.25-25	1.1×10^3	19
NiO-O_V	fluorescence	0.05-2	37.8	this work

Reference:

1. C. W. Lien, C. C. Huang and H. T. Chang, *Chem Commun.* 2012, **48**, 7952-7954.
2. T. Jin, Y. L. Li, W. J. Jing, Y. C. Li, L. Z. Fan and X. H. Li, *Chem Commun.* 2020, **56**, 659-662.
3. C. Song, W. Zhao, H. Liu, W. Ding, L. Zhang, J. Wang, Y. Yao and C. Yao, *J Mater Chem B.* 2020, **8**, 7494-7500.
4. P. C. Kuo, C. W. Lien, J. Y. Mao, B. Unnikrishnan, H. T. Chang, H. J. Lin and C. C. Huang, *Anal Chim Acta.* 2018, **1009**, 89-97.
5. C. W. Wu, B. Unnikrishnan, Y. T. Tseng, S. C. Wei, H. T. Chang and C. C. Huang, *J Colloid Interf Sci.* 2019, **541**, 75-85.
6. C. W. Lien, B. Unnikrishnan, S. G. Harroun, C. M. Wang, J. Y. Chang, H. T. Chang and C. C. Huang, *Biosens Bioelectron.* 2018, **102**, 510-517.
7. J. W. Wang, P. J. Ni, C. X. Chen, Y. Y. Jiang, C. H. Zhang, B. Wang, B. Q. Cao and Y. Z. Lu, *Microchim Acta.* 2020, **187**, 1-8.
8. J. J. Li, D. Qiao, J. Zhao, G. J. Weng, J. Zhu and J. W. Zhao, *Spectrochim Acta A.* 2019, **217**, 247-255.
9. X. F. Li, J. Qiao, Z. W. Li and L. Qi, *Analyst.* 2020, **145**, 2233-2237.
10. M. H. Zan, C. Li, D. M. Zhu, L. Rao, Q. F. Meng, B. Chen, W. Xie, X. W. Qie, L. Li, X. J. Zeng, Y. R. Li, W. F. Dong and W. Liu, *J Mater Chem B.* 2020, **8**, 919-927.
11. C. Wang, Y. X. Lan, F. Yuan, T. H. Fereja, B. H. Lou, S. Han, J. P. Li and G. B. Xu, *Microchim Acta.* 2020, **187**, 1-6.
12. W. H. Lu, J. Chen, L. S. Kong, F. Zhu, Z. Y. Feng and J. H. Zhan, *Sensor Actuat B-Chem.* 2021, **333**, 129560.
13. M. Singh, P. Weerathunge, P. D. Liyanage, E. Mayes, R. Ramanathan and V. Bansal, *Langmuir.* 2017, **33**, 10006-10015.
14. S. Hashmi, M. Singh, P. Weerathunge, E. L. H. Mayes, P. D. Mariathomas, S. N. Prasad, R. Ramanathan and V. Bansal, *Acs Appl Nano Mater.* 2021, **4**, 13352-13362.
15. C. Chen, Y. Wang and D. Zhang, *Microchim Acta.* 2019, **186**, 1-8.
16. B. Li, H. Chang, C. Wang and S. Wang, *Journal of Cluster Science.* 2021, **33**, 2463-2473.
17. C. Liu, Y. M. Zhao, D. Xu, X. X. Zheng and Q. Huang, *Anal Bioanal Chem.* 2021, **413**, 4013-4022.
18. S. Y. Feng, F. T. Wen, L. He, J. Y. Su, P. Jiang and D. P. He, *Sensor Actuat B-Chem.* 2022, **361**, 131745.
19. L. Y. Zhu, J. Zheng, Y. N. Ci, L. Han, J. J. Meng, J. Y. Qian and X. B. Yin, *Crystengcomm.* 2024, **26**, 1292-1302.